Poly(butyl terephthalate)/oxytetramethylene + oxidized carbon nanotubes hybrids: Mechanical and tribological behavior

Witold Brostow[a)]
Department of Materials Science and Engineering, Laboratory of Advanced Polymers and Optimized Materials; and Department of Physics, Center for Advanced Research and Technology, University of North Texas, Denton, Texas 76207

Georg Broza
Institute of Polymers and Composites, Technical University of Hamburg, 21073 Hamburg, Germany

Tea Datashvili and Haley E. Hagg Lobland
Department of Materials Science and Engineering, Laboratory of Advanced Polymers and Optimized Materials; and Department of Physics, Center for Advanced Research and Technology, University of North Texas, Denton, Texas 76207

Agata Kopyniecka
Institute of Polymers and Composites, Technical University of Hamburg, 21073 Hamburg, Germany

(Received 18 August 2011; accepted 20 March 2012)

We have created hybrids of functionalized single wall carbon nanotubes (fSWCNTs) and also multiwall CNTs (fMWCNTs) with PBT/PTMO, a block copolymer of semicrystalline poly(butyl terephthalate) (PBT) with amorphous oxytetramethylene (PTMO). For both single wall (SW) and multiwall (MW) carbon nanotubes (CNTs) tensile modulus and strain at break as a function of CNTs' concentration (c_{CNT}) show maxima. Elongation at break is enhanced by the nanotubes, a plasticizing effect—much stronger for SWCNTs because they have less contact points per unit area with the matrix and also are more flexible. Repetitive tensile tests were also performed; each loading cycle resulted in lowering the tensile modulus. Brittleness B(c_{CNT}) diagrams show minima. New results for CNT hybrids fit an earlier general diagram for determination of viscoelastic recovery in sliding wear (f) as a function of brittleness (B); the original equation with unchanged parameters covers also these results. Volumetric wear was determined after abrasion on a pin-on-disk tribometer. Minima are seen on the volumetric wear versus c_{CNT} diagrams, similar to those on the B(c_{CNT}) diagrams.

I. INTRODUCTION

Poly(ether-b-ester) copolymers have numerous applications as engineering materials due to their attractive combination of strength, high elasticity, melt stability and high crystallization rates. These elastomers are block copolymers that contain alternatively crystallizable (hard) and noncrystallizable (soft) chain segments, resulting in a material with high melting temperature crystallites (hard segments)—dispersed in a soft component and low glass transition temperature matrix. High melting temperatures are pertinent in quest for polymers, which can survive temperature cycling over wide temperature ranges for applications in thermoelectric (TE) devices.[1,2] Our segmented poly(ether-b-ester) copolymers of poly(butyl terephthalate) (PBT) and oxytetramethylene (PTMO) belong to the family of such thermoplastic elastomers.[3] The nanometric structure of segregated hard and soft segments is mainly responsible for the outstanding mechanical properties of these materials.[4]

Generally and as well known, properties of polymers can be modified and improved by addition of fillers with sizes in the nm range[5–19] including carbon nanotubes (CNTs).[20–33] CNTs exhibit a high elastic modulus, strong electrical and high thermal conductivity. CNTs are an appreciated filler material for creation of composites due to unique or advantageous properties they impart to polymers.

Most of the literature on CNT-containing composites does not deal with tribological properties. This lack of investigations into the tribological properties should be seen in the context of eloquent discussions of Rabinowicz[34] on the huge losses suffered by industry caused by scratchability and wear of various kinds. In this work we have studies tribological and mechanical properties—looking for connections between them. We recall that in 2006 when some of us defined brittleness B[35] we have also connected it to the viscoelastic recovery f in sliding wear determination. Subsequent work has shown that our B(f) relationship applies to

[a)]Address all correspondence to this author.
e-mail: wbrostow@yahoo.com
DOI: 10.1557/jmr.2012.116

even more polymers and polymer-based composites.[36,37] In this work we are looking at even more connections between mechanical and tribological properties.

We have applied both single wall CNTs (SWCNTs) and multiwall CNTs (MWCNTs) subjecting them to a functionalization process. We have developed a method of making nanohybrids from oxidized CNTs in copolymer matrices by using an in situ polycondensation process. Such a process was first introduced for multiblock copoly(ether-*b*-ester)s based on semicrystalline PBT blocks with amorphous PTMO blocks.[27] The name nanohybrids is more specific than nanocomposites since it includes the fact that the former involve both inorganic and organic constituents; by contrast, a nanocomposite can for instance consist of nanoparticles of a metal in a ceramic and thus be fully inorganic. The level of nanotube aggregation within the polymer matrix depends on the procedure followed to synthesize the PBT/PTMO with CNT nanohybrid. A better dispersion can be achieved when CNTs are added to dimethyl terephthalate (DMT) + butanediol (BD) monomers before transesterification.[28] We have decided to explore among others whether CNTs can improve tribological properties of PBT/PTMO.

II. EXPERIMENTAL AND MATERIALS

A. Synthesis of carbon nanotubes

We have used high-purity and high-quality CNTs. SWCNTs were supplied by CNI Technology Co., Norman, OK, synthesized by the HIPCO method.[30] According to the manufacturer, the diameter of the SWCNTs was from 0.6 to 1.8 nm with the length of several μm and purity >97 wt%. Thin MWCNTs were supplied by Nanocyl S.A., Sambreville, Belgium, synthesized using chemical vapor deposition (CVD) technique.[30] The average diameter of the MWCNTs was about 10 nm with the length of 10–50 μm.

B. Functionalization of carbon nanotubes

There is a diversity of chemical reactions that can modify the surfaces of CNTs.[30] To achieve a good dispersion of CNTs in the polymeric matrix and strong interface adhesion, the surfaces of CNTs should be chemically functionalized.[29] Kopczynska and Ehrenstein discuss the importance of interfaces for properties of multiphase composites.[38] Chemical modification of filler can even produce lowering of viscosity of the melt as compared with the neat molten polymer without filler.[39] The typical tendency is the opposite, that is, a viscosity increase caused by the filler.

The process of functionalization of CNTs consists of the following three steps. The first step is oxidation. In our case, 4.1 g of CNTs were put into 200 mL distilled water and the suspension introduced into a three-necked flask placed in an oil bath. Thereafter, 200 mL of 65% aq. nitric acid were added, thus in the 1:1 proportion. The mixture was slowly heated up to 100 °C under ambient pressure and constant mixing to render a homogeneous dispersion. Helium gas was used to entrain gases formed during the reaction. This reaction took 20 h.

In the second stage we first turned off the heating. 300 mL of dimethyl sulfoxide (DMSO) and 10 mL thionyl chloride were added very slowly to the reaction mixture. The second step took 20 additional hours. Afterward, 20 mL of N,N-dimethylformamide and 8 mL of butylene glycol (1,4-butanediol) were mixed together in a beaker and this composition was added to the flask (step 3). The temperature was maintained around 80 °C and then our mixture was left for 24 h. Afterward, we had washed carbon nanotubes in a suction flask with N,N-dimethylformamide until pH ≈ 7 was reached. The expected result was functionalization of the surfaces of the CNTs.

C. Reaction of functionalized CNTs with PBT/PTMO copolymers

As described in Ref. 3, one can create block copoly (ether-b-ester)s based on semicrystalline hard segments of PBT and amorphous soft segments of PTMO. Such block copolymers were treated with varying amounts of functionalized CNTs in a two-stage process. Thus, DMT, BD, functionalized carbon nanotubes (fCNTs) dispersed in BD + DMT and the catalyst were poured into a reactor and mixed (90 rpm) at 175 °C under normal pressure. The second step was polycondensation when liquid PTMO and a stabilizer were added (250 °C, 40 rpm). Then the pressure was reduced to 50 Pa. These processes result in formation of two by-products: methanol (transesterification) and butylene glycol (polycondensation). Progress of functionalization has been followed by Raman spectroscopy but we have not included those results in this article for brevity's sake. We note that Raman spectroscopy does not discriminate between functionalization types.

D. Microscopy

We have used a LEO Gemini 1530 scanning electron microscope (SEM; Oberkochen, Germany). Samples were fractured in liquid nitrogen. A range of accelerating voltages, 3–10 kV, was applied. Because of the low conductivity of the specimens, a thin layer of gold was sputtered onto the surfaces, with the thickness of the gold layer ≈ 10 nm. This in turn enabled the use of low beam energies.

E. Tensile testing

Specimens were prepared by injection molding. The DIN EN ISO 527-2 standard was followed. A Zwick universal testing machine (Ulm, Germany) was used. The tests were conducted at the rate of 25 mm/min while the starting clamp distance was 32 mm. Young's modulus

was calculated for the elongation range between 0.05—0.25% at a constant crosshead rate of 25 mm/min. Five tests have been made for each type of samples; we report averages here.

F. Dynamic mechanical analysis (DMA)

DMA testing was performed using a PerkinElmer DMA7 machine (Waltham, MA). Specimens were analyzed in rectangular form using a three-point bending fixture in the temperature T scan mode from 25 °C to 170 °C at the heating rate of 3 K/min. The frequency applied was 1.0 Hz. We have recorded the storage (solid-like) modulus E′, the loss (liquid-like) modulus E′′ and tan $\delta = E''/E'$.

G. Scratch resistance and sliding wear

Scratch tests were carried out on tensile test specimens using a CSM microscratch tester (Peseux, Switzerland) with a conical diamond indenter (200 mm diameter and 120° cone angle) following the procedure described in review articles.[40,41] Both single scratches and sliding wear testing (= 15 scratches along the same groove) were performed under the following conditions: normal load 5.0, 10.0, 15.0 and 20.0 N; scratch length 5.0 mm, 5.0 mm/min scratch speed at room temperature (25 °C). For each test, the instantaneous penetration depth R_p and the residual depth R_h after healing were recorded. R_h values have in each case been determined 2 min after recording the R_p values–sufficient time for full recovery to occur. The percentage of viscoelastic recovery f was calculated from R_p and R_h for the 15th scratch as

$$f = [1 - (R_h/R_p)]\,100\% \quad . \tag{1}$$

H. Volumetric wear

For determination of the wear and wear mechanisms of these materials, a Nanovea series pin–on–disk tribometer from Microphotonics Inc. (Allentown, PA) was used. Using a stainless steel ball, tests were conducted for 50 min, at 100 revolutions per min, thus up to 5000 revolutions. The force applied was 5.0 N at ≈21 °C.

Cross-section areas of wear tracks remaining after the pin–on–disk tribometry were determined using a Veeco Dektak 150 profilometer.

The wear volume V_m of the tracks produced by the pin–on–disk testing was determined using the average cross-sectional area A_m obtained from the profilometer. The obtained cross-section area is multiplied by wear track length, namely

$$V_m = 2\pi R_m A_m \quad , \tag{2}$$

where R_m is the radius of the wear track. The wear rate is then calculated as

$$Z = V_m/(Wx) \quad . \tag{3}$$

Here W is the normal load while x is the sliding distance.

III. MICROSCOPY RESULTS

Scanning electron micrographs of PBT/PTMO nanohybrids with 0.5 wt% of fMWCNTs and with 0.3 wt% of fSWCNTs are presented in Fig. 1. In both cases a fairly homogeneous distribution of the CNTs in the PBT/PTMO matrix, which is produced by the in situ polycondensation, is seen. The results shown are representative of all the nanohybrids prepared.

IV. TENSILE TESTING AND CYCLIC STRESSING RESULTS

Consider first results for SWCNTs. Results of mechanical testing for pure PBT/PTMO and for nanohybrids with varying amounts of fSWCNTs are presented in Table I. The corresponding stress versus strain diagrams are shown in Fig. 2 (top).

A comparison of the Young's modulus values for the different compositions is shown in Fig. 2 (bottom). We have: for neat copolymer E = 83 MPa, for 0.1% CNTs is E = 96.4 MPa, for 0.2% CNTs is E = 97.5 MPa. At 0.2 wt% of CNTs there is a maximum, at higher CNT concentrations the modulus decreases—but it is still higher

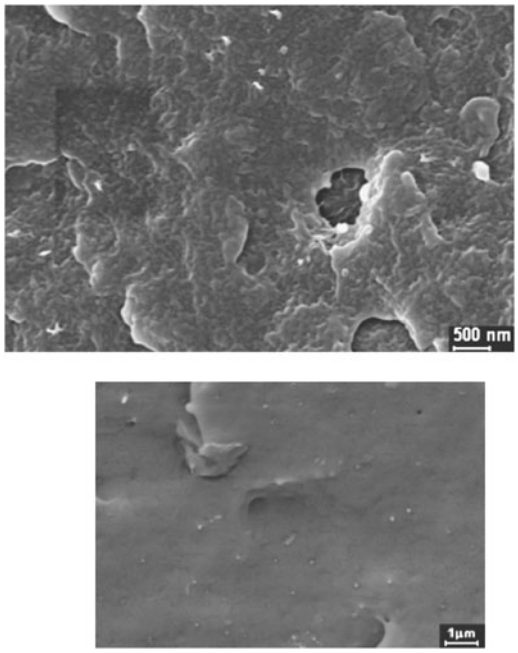

FIG. 1. SEM micrographs of fracture surfaces of the PBT/PTMO nanohybrids with 0.5 wt% fMWCNTs (top) and of the nanohybrids with 0.3 wt% fSWCNTs (bottom), in both cases with a gold layer of 10 nm thickness.

TABLE I. Summary of tensile properties of PBT/PTMO block copolymers with fSWCNTs.

Material	Young's modulus E/*MPa*	Stress at break σ_b/*MPa*	Strain at break ε_b/%
PBT/PTMO	83.0	34.8	596
PBT/PTMO + 0.1 wt% fSWCNTs	96.4	30.1	697
PBT/PTMO + 0.2 wt% fSWCNTs	97.5	31.0	719
PBT/PTMO + 0.3 wt% fSWCNTs	86.8	30.6	768
PBT/PTMO + 0.5 wt% fSWCNTs	87.0	29.6	683

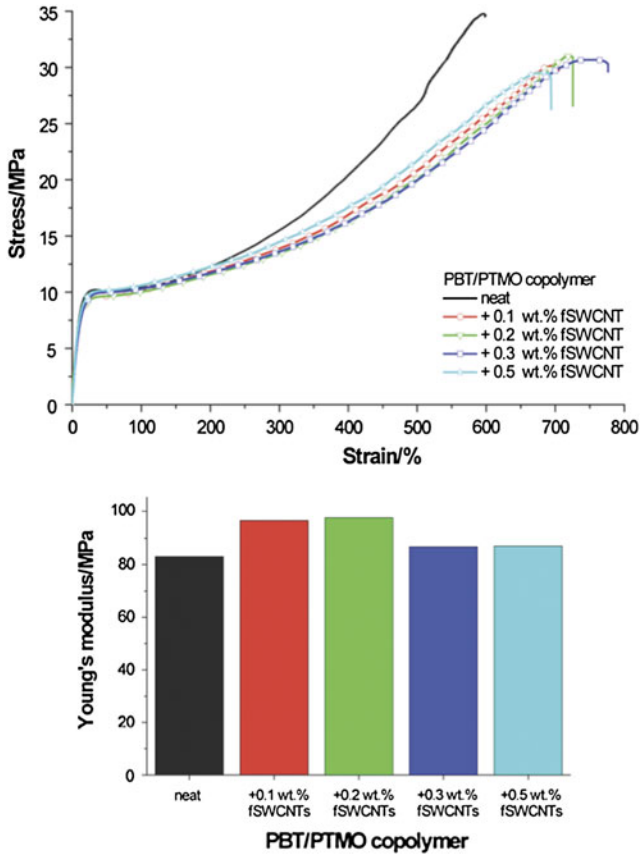

FIG. 2. Stress versus strain curves for neat PBT/PTMO and PBT/PTMO nanohybrids with different amounts of fSWCNTs (top); also the respective Young's modulus (bottom).

than for the neat copolymer. Among the nanohybrids the lowest value E = 87 MPa is for 0.5 wt% CNTs, only 4 MPa higher than for pure copolymer. At E = 86.7 MPa, the value for 0.3% CNTs is virtually the same as for 0.5% CNTs.

Aggregation of CNTs taking place at higher concentrations cannot be excluded. To explain results in Fig. 2 above, we have to consider at least two more effects. As expected, more CNTs should give more reinforcement. At the same time, more CNTs result in less cohesion in the matrix. We recall a discussion by Pisanova and Zhandarov[42] about the behavior of cylindrical or fiber-shaped reinforcement under load. The stress imposed can lead to local debonding of the fiber from the matrix—starting at the fiber ends. More CNTs provide more nanotube ends where debonding can begin. A combined result of these effects is a maximum of E. We note also the results of Szymczyk et al.[43] on poly(trimethylene terephthalate) + MWCTNs materials. These authors report maxima of tensile modulus, of tensile stress at break and of storage modulus in dynamic mechanical testing as a function of CNTs concentration.

The elongation at break is the highest for PBT/PTMO with 0.3 wt% fSWCNTs and has the value of 768%, which is more than 170% higher than for the neat copolymer.

The highest stress at break σ_b is for the neat copolymer, ≈35 MPa. It is about 16% higher than for our nanohybrids. By contrast, the strain at break ε_s is larger for nanohybrids than for the neat copolymer. Thus, the functionalized single-walled CNTs in nanohybrids provide a plasticization effect.

We now consider the nanohybrids containing fMWCNTs. Numerical data are presented in Table II. The respective stress versus strain curves are shown in Fig. 3 (top). Young's modulus values are compared in Fig. 3 (bottom).

We see an increase of Young's modulus for nanohybrids with fMWCNTs compared with the neat copolymer. The values are about 20% higher than for nanohybrids containing fSWCNTs. Thus, MW tubes provide more reinforcement—as expected. The highest stress at break σ_b is for 0.2 wt% CNTs (40.5 MPa).

The strain at break values are not as high as for nanohybrids with SWCNTs, in the range 580–610%, approximately 100% lower than in SWCNTs systems. Thus, there is a plasticizing effect but a much weaker one than for single-wall nanotubes. We have already quoted the discussion by Kopczynska and Ehrenstein[38] on the role of interfaces in properties of multiphase polymer-based materials. Consider now the effects of tensile force application on our nanohybrids. SWCNTs have smoother surfaces than MWCNTs. Thus, polymeric chains slide along SW nanotube surfaces fairly easily, hence plasticization. MW nanotubes also provide some sliding capability to the chains—but less than SW tubes. Consider contact points between the chains and the nanotube surfaces. Whether one considers the so-called parchment model of MW tubes or the so-called Russian doll model of these tubes, in general the MW tubes have more contact points per unit surface area than SW tubes. These points offer resistance to chain movements. While the contact point model is appealing, there is no experimental procedure for determination of their numbers per unit surface area. Possibly future molecular dynamics simulations of multiphase polymers subjected to external forces[44,45]

TABLE II. Summary of tensile properties of PBT/PTMO block copolymers with fMWCNTs.

Material	Young's modulus *E*/*MPa*	Stress at break σ_b/*MPa*	Strain at break ε_b/%
PBT/PTMO	83.0	34.8	596
PBT/PTMO + 0.1 wt% fMWCNTs	115.3	35.0	608
PBT/PTMO + 0.2 wt% fMWCNTs	116.3	40.5	612
PBT/PTMO + 0.5 wt% fMWCNTs	116.8	33.3	617

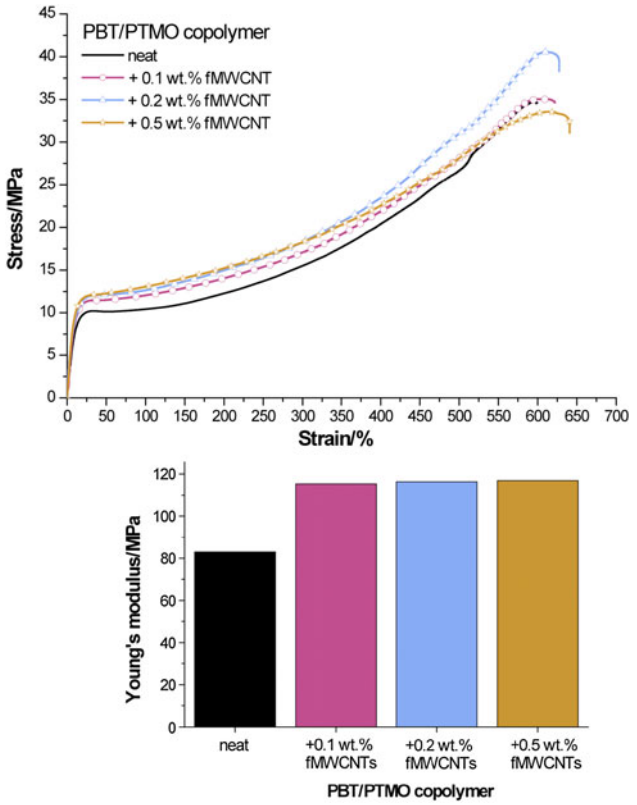

FIG. 3. Stress versus strain curves for neat PBT/PTMO and PBT/PTMO nanohybrids with different amounts of fMWCNTs (top); also the respective Young's modulus (bottom).

might provide a way of dealing with this model. We also note that SW tubes are more flexible than MW tubes, hence one more reason for a stronger plasticization effect provided by the former.

We have also performed repetitive or cyclic tensile stressing tests. Examples are shown in Fig. 4 for 0.1 wt% of fSWCNTs and for the same concentration of fMWCNTs.

In general, multiple loading provides results similar to and confirming those from one-time tensile testing. Thus, MW tubes provide more reinforcement. This, while SW tubes provide more plasticization, hence higher strain values. We see that each loading cycle results in "lowering"

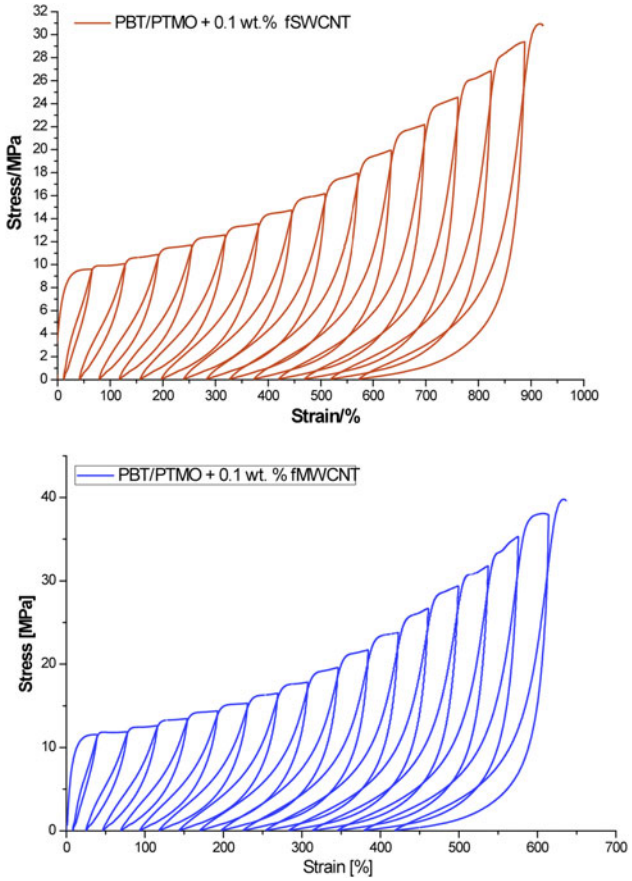

FIG. 4. Results of repetitive tensile cycling: (a) 0.1 wt% fSWCNTs and (b) 0.1 wt% fMWCNTs.

the tensile modulus. We summarize cycling loading results in Fig. 5. There is a dramatic drop in E during the first few cycles for each composition for both SW and MW nanotubes.

V. SCRATCH TESTING AND SLIDING WEAR RESULTS

We show in Fig. 6 sliding wear results as penetration (instantaneous) depth R_p and residual (healing) depth R_h values for fSWCNTs at the load of 20.0 N. We recall that the consecutive passes of the indenter go along the original groove created during the pass number 1. Results for other loads and for fMWCNTs are omitted for brevity's sake. However, we note that—as expected—smaller R_p and R_h depths are seen under lower loads. Larger differences between samples of different compositions are seen at higher loads. SW tubes provide between 2 and 3% higher viscoelastic recovery f values; see again Eq. (1). This confirms the hypothesis of more plasticization by SW nanotubes than by MW tubes—already used to explain results of one-time tensile testing and also of cyclic loading. We shall return to the f results later in this article.

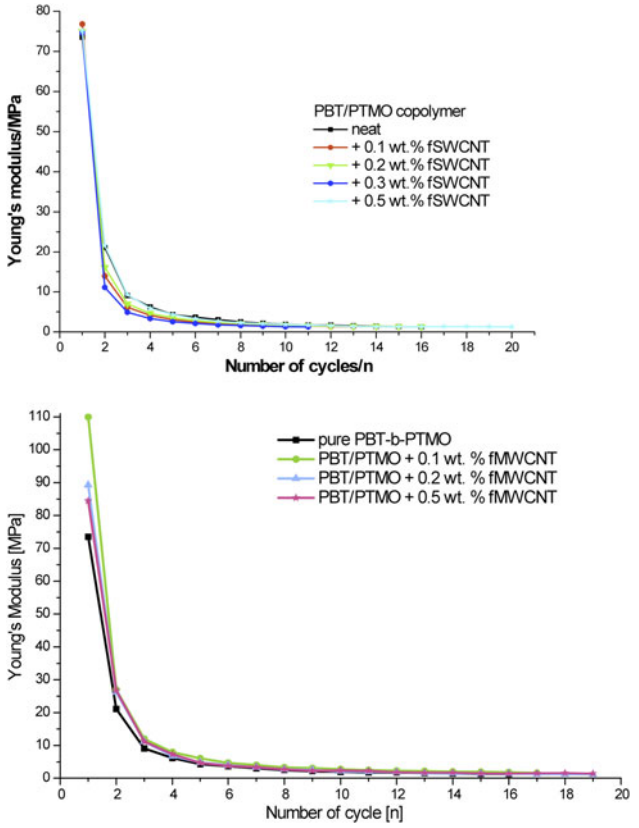

FIG. 5. Variation of Young's modulus as a result of the number of load cycles: (top) fSWCNTs; (bottom) fMWCNTs.

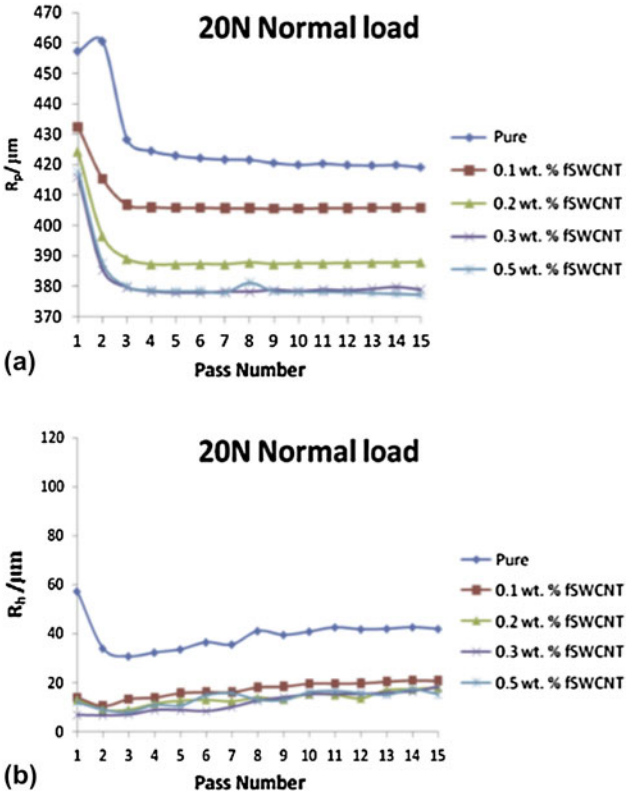

FIG. 6. Sliding wear results as a function of the pass number: (a) penetration depths R_p and (b) residual healing depths R_h for 20.0 N.

We see in Fig. 6 that strain hardening in sliding wear discovered before[46] takes place in these materials also. Most polymers and polymer-based composites investigated so far exhibit this phenomenon. Polystyrene does not, a fact that has led to the definition of brittleness of materials:[35]

$$B = \frac{1}{E' \cdot \varepsilon_b} \quad . \tag{4}$$

A combined discussion of B and viscoelastic recovery f will be provided in Sec. VI.

VI. DYNAMIC MECHANICAL ANALYSIS AND BRITTLENESS

Values of B calculated from Eq. (4) are displayed in Tables III and IV for SWCNT and MWCNT hybrids, respectively.

We now present in Fig. 7 values of f as a function of B calculated from the formula[35]

$$f = 30.6 + 67.1\, e^{-B/0.505} \quad . \tag{5}$$

Brittleness is, of course, an aspect commonly considered in evaluating materials' performance. Using a combination of parameters obtained from dynamic and quasistatic testing methods, brittleness has been defined quantitatively by Eq. (4), providing a measure for comparability of different materials.[35] Values of the parameters used to calculate B, the strain at break and storage modulus, are reported in Tables III–V. Importantly, brittleness has been correlated with several other properties,[35–37,43] including to viscoelastic recovery in sliding wear (f). The correlation between B and f has been tested for a variety of neat polymers, including homopolymers and copolymers, thermoplastics

TABLE III. Summary of brittleness and viscoelastic recovery results for fSWCNT hybrids.

Material	Viscoelastic recovery *f*/%	Storage modulus at 25°C *E'*/*Pa*	Brittleness *B*
PBT/PTMO	90.0	90.0	1.86 E-05
PBT/PTMO + 0.1 wt% fSWCNTs	94.9	130.7	1.10 E-05
PBT/PTMO + 0.2 wt% fSWCNTs	95.4	139.9	0.99 E-05
PBT/PTMO + 0.3 wt% fSWCNTs	95.2	142.7	0.91 E-05
PBT/PTMO + 0.5 wt% fSWCNTs	96.0	142.2	1.03 E-05

and elastomers as well as for several composites with nano- and micropowder additives, metals and ceramics. Consequently, it is evident that B is an appropriate descriptor for all types of polymer-based materials and that the relationship between B and f is not limited in the use to neat polymers only. The essential diagram shown in Fig. 7 was defined at the time brittleness was defined[35] and the parameters in Eq. (5) are original ones. Importantly, we see that the points now obtained for our nanohybrids and for PBT/PTMO fit the general curve. There are two outliers as before: polymethyl methacrylate (PMMA) and styrene/acrylonitrile copolymer (SAN). The data for those materials come from some websites and were used in default of more accurate ones. Our present nanohybrids have brittleness slightly higher than the unmodified PBT/PTMO; however B values go through a minimum around 0.3% of fSWCNTs and around 0.3% of fMWCNTs. We recall again results of Szymczyk et al.[43] who report also a minimum of brittleness as a function of CNTs' concentration.

TABLE IV. Summary of brittleness and viscoelastic recovery results for fMWCNT hybrids.

Material	Viscoelastic recovery *f*/%	Storage modulus at 25 °C *E'*/*Pa*	Brittleness *B*
PBT/PTMO	90.0	90.0	1.86 E-05
PBT/PTMO + 0.1 wt% fMWCNTs	95.1	131.2	1.25 E-05
PBT/PTMO + 0.2 wt% fMWCNTs	92.7	137.6	1.19 E-05
PBT/PTMO + 0.3 wt% fMWCNTs	94.0	140.3	1.16 E-05
PBT/PTMO + 0.5 wt% fMWCNTs	92.1	138.6	1.17 E-05

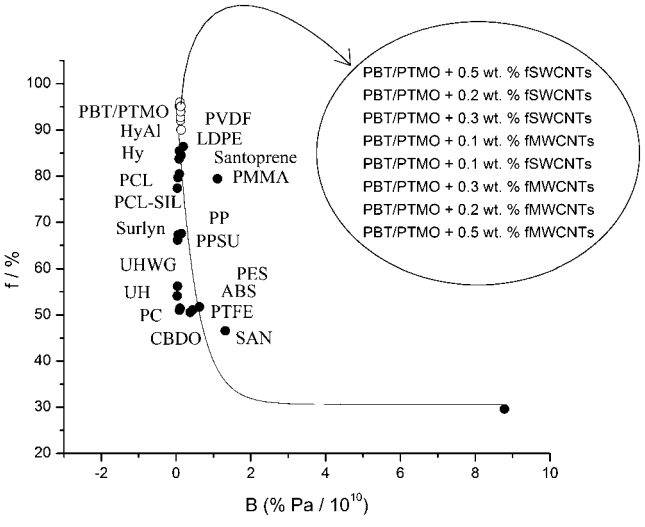

FIG. 7. Viscoelastic recovery in sliding wear (f) as a function of brittleness (B). Points for materials other than those studied in this work are from.[35–37]

VII. VOLUMETRIC WEAR

There are several mechanisms of wear[41,47] and different types of wear occur under different conditions. In this section, we report results of abrasive determination performed using a pin-on-disk tribometer and resulting in volumetric wear. One thus evaluates the volume of the debris formed. By contrast, in microscratch testing and sliding wear determination reported above in Sec. V there can be very little or no debris. As discussed earlier, the indenter leaves behind a groove and two top ridges along the groove.[48] We summarize the volumetric wear results for SWCNTs and MWCNTs in Tables V and VI respectively and in Fig. 8.

We see minima on the diagrams for both single-wall and multiwall CNTs. We recall that the values of B as a function of c_{CNT} presented in Tables III and IV also exhibit minima. A possible joint explanation of these results is in terms already discussed in Sec. IV when talking about the tensile modulus and strain at break: a competition between the reinforcing effect of the nanotubes and lowering the cohesion of the polymeric matrix by the presence of the nanotubes. We intend to pursue a relationship between volumetric wear (Z) and brittleness (B) and report the results in a later publication. We recall the results of Vail, Burris and Sawyer[33] for polytetrafluoroethylene (PTFE) + SWCNTs: wear rates determined from volume loss as a function of c_{CNT} show a minimum. CNTs concentrations used in that study are much higher than ours, presumably because PTFE does not 'cooperate with anything'. We note that the existence of extrema on diagrams of material properties as a function of CNTs concentration is by no means automatic.

VIII. A SURVEY OF RESULTS

Kopczynska and Ehrenstein[38] as well as Desai and Kapral[49] note the importance of interfaces for properties of multiphase materials. While processing can affect properties of polymers[50] and polymer-based composites[51]

TABLE V. Summary of wear results for SWCNTs containing hybrids.

Material	Wear rate *Z*/(mm^3/(*m***s*))
PBT/PTMO	180 E-05
PBT/PTMO + 0.1 wt% fSWCNTs	161 E-05
PBT/PTMO + 0.3 wt% fSWCNTs	169 E-05

TABLE VI. Summary of wear results for MWCNTs containing hybrids.

Material	Wear rate *Z*/(mm^3/(*m***s*))
PBT/PTMO	180 E-05
PBT/PTMO + 0.1 wt% fMWCNTs	146 E-05
PBT/PTMO + 0.2 wt% fMWCNTs	128 E-05
PBT/PTMO + 0.5 wt% fMWCNTs	179 E-05

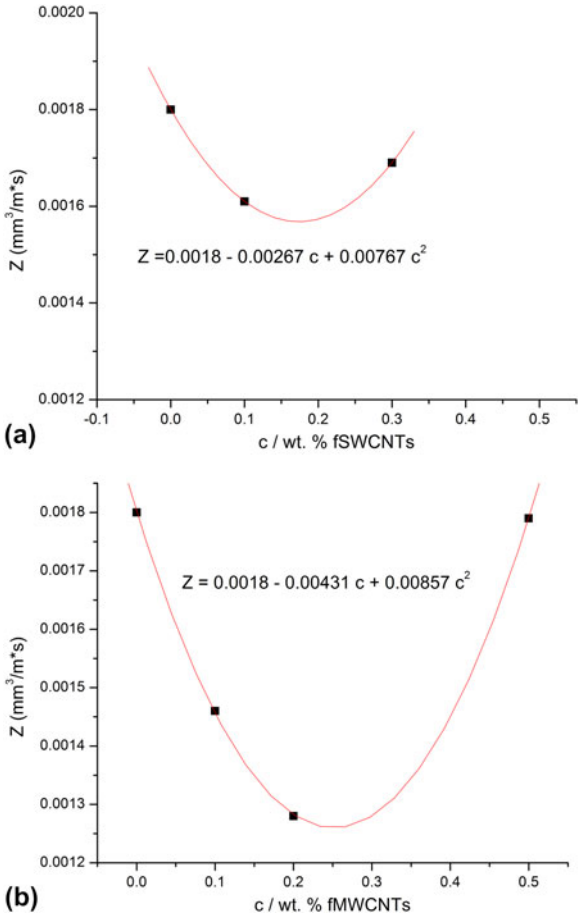

FIG. 8. Volumetric wear Z as a function of the concentration of nanotubes c_{CNT}: (a) single wall tubes and (b) multiwall tubes.

significantly, the role of interfaces comes out clearly in our results. Reinforcement of a polymeric matrix does not necessarily improve properties proportionately to the filler concentration, c_{CNT} in our case. We have found out the double-edge sword effect of our carbon nanotubes. On one hand, we see the reinforcement effect. On the other, the nanotubes constitute a 'foreign body' weakening the continuity and cohesion of the polymeric matrix. We have reported above minima on the brittleness B versus c_{CNT} diagrams—both for single wall and multiwall CNTs—a consequence of these two effects acting simultaneously. Similarly, we have found minima on the wear $Z(c_{CNT})$ diagrams, again for both SWCNTs and MWCNTs. Our results reinforce the conclusion that a nanohybrid with a high concentration of the nanofiller by no means guarantees a large desired improvement of polymer properties.

We have noted above potential use of high temperature polymers with reinforcing fillers in thermoelectric devices. Electrodes in organic solar cells can be made using CNTs—provided approximately parallel orientation of the nanotubes can be achieved.[52]

ACKNOWLEDGMENTS

We appreciate discussions with Olena Astahova, Michael Bratychak, Volodymyr Donchak and Olena Shyshchak, all at the Lvivska Politechnika National University. Partial financial support was provided by the II-VI Foundation, Bridgeville, PA.

REFERENCES

1. H.J. Goldsmid: *Thermoelectric Refrigeration* (Plenum Press, New York, 1964).
2. D.M. Rowe: *Thermoelectrics Handbook—Macro to Nano* (Taylor and Francis, New York, 2006).
3. G. Broza and K. Schulte: Orientation behavior in axial tension of half-molten poly(ether-b-ester) copolymers, in *Block Copolymers*, edited by F.J. Baltá Calleja and Z. Roslaniec (Marcel Dekker, New York, 2000); pp. 434, Chapter 15.
4. H. Schroeder and R.J. Cella: *Encyclopedia of Polymer Science and Engineering* (Wiley, New York, 1988), Chapter 12.
5. M. Rabello: *Additives for Polymers* (Artliber, São Paulo, 2000).
6. K.G. Gatos, R. Thomann, and J. Karger-Kocsis: Characteristics of ethylene propylene diene monomer rubber/organoclay nanohybrids resulting from different processing conditions and formulations. *Polym. Int.* **53**, 1191 (2004).
7. D.S. dos Santos, Jr., P.J.G. Goulet, N.P.W. Pieczonka, O.N. Oliveira, Jr., and J.R. Aroca: Gold nanoparticle embedded, self-sustained chitosan films as substrates for surface-enhanced Raman scattering. *Langmuir*. **20**, 10273 (2004).
8. W. Brostow, M. Keselman, I. Mironi-Harpaz, M. Narkis, and R. Peirce: Effects of carbon black on tribology of blends of poly (vinylidene fluoride) with irradiated and non irradiated ultrahigh molecular weight polyethylene. *Polymer*. **46**, 5058 (2005).
9. W.S. Chow, Z.A. Mohd Ishak, and J. Karger-Kocsis: An atomic force microscopy study on the blend morphology and clay dispersion in Polyamide-6 polypropylene/organoclay system. *J. Polym. Sci., Part B: Polym. Phys.* **43**, 1198 (2005).
10. W. Brostow, B.P. Gorman, and O. Olea-Mejia: Focused ion beam milling and scanning electron microscopy characterization of polymer + metal hybrids. *Mater. Lett.* **61**, 1333 (2007).
11. K.G. Gatos, K. Kameo, and J. Karger-Kocsis: On the friction and sliding wear of rubber/layered silicate nanohybrids. *Express Polym. Lett.* **1**, 27 (2007).
12. W. Brostow, A. Buchman, E. Buchman, and O. Olea-Mejia: Microhybrids of metal powder incorporated in polymeric matrices: Friction, mechanical behavior, and microstructure. *Polym. Eng. Sci.* **48**, 1977 (2008).
13. J. Karger-Kocsis, P.P. Shang, Z.A. Mohd Ishak, and M. Rösch: Melting and crystallization of in situ polymerized cyclic butylene terephthalates with and without organoclay: A modulated DSC study. *Express Polym. Lett.* **1**, 60 (2007).
14. A. Pegoretti, A. Dorigato, and A. Penati: Tensile mechanical response of polyethylene-clay nanohybrids. *Express Polym. Lett.* **1**, 123 (2007).
15. W. Brostow, T. Datashvili, and K.P. Hackenberg: Synthesis and characterization of poly(methyl acrylate) + SiO_2 hybrids. e-Polymers no. 054 (2008).
16. F.J. Carrión, A. Arribas, M-D. Bermúdez, and A. Guillamon: Physical and tribological properties of a new polycarbonate-organoclay nanohybrids. *Eur. Polym. J.* **44**, 968 (2008).
17. L.D. Perez, L.F. Giraldo, W. Brostow, and B.L. Lopez: Poly(methyl acrylate) + mesoporous silica nanohybrids: Mechanical and thermophysical properties. e-Polymers no. 029 (2007).

18. A. Arribas, M-D. Bermudez, W. Brostow, F-J. Carrion-Vilches, and O. Olea-Mejia: Scratch resistance of a polycarbonate + organoclay nanohybrid. *Express Polym. Lett.* **3**, 621 (2009).
19. W. Brostow, W. Chonkaew, T. Datashvili, and K.P. Menard: Tribological properties of epoxy + silica hybrid materials. *J. Nanosci. Nanotechnol.* **9**, 1916 (2009).
20. O. Lourie and H.D. Wagner: Evaluation of Young's modulus of carbon nanotubes by micro-Raman spectroscopy. *J. Mater. Res.* **13**, 2418 (1998).
21. H.D. Wagner, O. Lourie, Y. Feldman, and R. Tenne: Stress-induced fragmentation of multiwall carbon nanotubes in a polymer matrix. *Appl. Phys. Lett.* **73**, 3527 (1998).
22. J. Sandler, M.S.P. Shaffer, T. Prasse, W. Bauhofer, K. Schulte, and A.H. Windle: Development of a dispersion process for carbon nanotubes in an epoxy matrix and the resulting electrical properties. *Polymer* **40**, 5967 (1999).
23. M. Su, B. Zheng, and J. Liu: A scalable CVD method for the synthesis of single-walled carbon nanotubes with high catalyst productivity. *Chem. Phys. Lett.* **322**, 321 (2000).
24. Z. Roslaniec, G. Broza, and K. Schulte: Nanohybrids based on multiblock polyester elastomers (PEEs) and carbon nanotubes (CNTs). *Compos. Interfaces* **10**, 95 (2003).
25. A. Assouline, A. Lustiger, A.H. Barber, C.A. Cooper, E. Klein, E. Wachtel, and H.D. Wagner: Nucleation ability of multiwall carbon nanotubes in polypropylene composites. *J. Polym. Sci., Part B: Polym. Phys.* **41**, 520 (2003).
26. Y. Ando, X. Zhao, T. Sugai, and M. Kumar: Growing carbon nanotubes. *Mater. Today* **7**, 22 (2004).
27. G. Broza, M. Kwiatkowska, Z. Roslaniec, and K. Schulte: Processing and assessment of poly(butylene terephthalate) nanohybrids reinforced with oxidized single wall carbon nanotubes. *Polymer* **46**, 5860 (2005).
28. G. Broza: Thermoplastic elastomers with multiwalled carbon nanotubes: Influence of dispersion methods on morphology. *Compos. Sci. Technol.* **70**, 1006 (2010).
29. X-L. Xie, Y-W. Mai, and X-P. Zhou: Dispersion and alignment of carbon nanotubes in polymer matrix. *Mater. Sci. Eng., R* **49**, 89 (2005).
30. G. Broza: Synthesis, properties, functionalization and applications of carbon nanotubes: A state of the art review. *Chem. Chem. Technol.* **4**, 35 (2010).
31. L.F. Giraldo, W. Brostow, E. Devaux, B.L. López, and L.D. Pérez: Scratch and wear resistance of Polyamide 6 reinforced with multiwall carbon nanotubes. *J. Nanosci. Nanotechnol.* **8**, 3176 (2008).
32. L.F. Giraldo, B.L. López, and W. Brostow: Effects of the type of carbon nanotubes on tribological properties of Polyamide 6. *Polym. Eng. Sci.* **49**, 896 (2009).
33. J.R. Vail, D.L. Burris, and W.G. Sawyer: Multifunctionality of single-walled carbon nanotube–polytetrafluoroethylene nanocomposites. *Wear* **267**, 619 (2009).
34. E. Rabinowicz: *Friction and Wear of Materials*, 2nd ed. (Wiley, New York, 1995).
35. W. Brostow, H.E. Hagg Lobland, and M. Narkis: Sliding wear, viscoelasticity and brittleness of polymers. *J. Mater. Res.* **21**, 2422 (2006).
36. W. Brostow and H.E. Hagg Lobland: Brittleness of materials: Implications for composites and relation to impact strength. *J. Mater. Sci.* **45**, 242 (2010).
37. W. Brostow, H.E. Hagg Lobland, and M. Narkis: The concept of materials brittleness and its applications. *Polym. Bull.* **59**, 1697 (2011).
38. A. Kopczynska and G.W. Ehrenstein: Polymeric surfaces and their true surface tension in solids and melts. *J. Mater. Educ.* **29**, 325 (2007).
39. P. Blaszczak, W. Brostow, T. Datashvili, and H.E. Hagg Lobland: Rheology of low-density polyethylene + Boehmite composites. *Polym. Compos.* **31**, 1909 (2010); Idem, http://4spepro.org/view.php?source=003493-2011-01-11.
40. W. Brostow, J-L. Deborde, M. Jaklewicz, and P. Olszynski: Tribology with emphasis on polymers: Friction, scratch resistance and wear. *J. Mater. Educ.* **25**, 119 (2003).
41. W. Brostow, V. Kovacevic, D. Vrsaljko, and J. Whitworth: Tribology of polymers and polymer-based composites. *J. Mater. Educ.* **32**, 273 (2010).
42. E. Pisanova and S. Zhandarov: Fiber-reinforced heterogeneous composites, in *Performance of Plastics*, edited by W. Brostow (Hanser, Munich—Cincinnati, 2000), Chapter 19.
43. A. Szymczyk, Z. Roslaniec, M. Zenker, M.C. Garcia-Gutierrez, J.J. Hernandez, D.R. Rueda, A. Nogales, and T.A. Ezquerra: Preparation and characterization of nanohybrids based on COOH functionalized multiwalled carbon nanotubes and on poly(trimethylene terephthalate). *Express Polym. Lett.* **5**, 977 (2011).
44. W. Brostow, A.M. Cunha, J. Quintanilla, and R. Simões: Predicting cracking phenomena in molecular dynamics simulations of polymer liquid crystals. *Macromol. Theory Simul.* **11**, 308 (2002).
45. W. Brostow and R. Simões: Tribological and mechanical behavior of polymers simulated by molecular dynamics. *J. Mater. Educ.* **27**, 19 (2005).
46. W. Brostow, G. Damarla, J. Howe, and D. Pietkiewicz: Determination of wear of surfaces by scratch testing. e-Polymers, no. 025 (2004).
47. N.K. Myshkin, M.I. Petrokovets, and A.V. Kovalev, Tribology of polymers: Friction, wear and mass transfer. *Tribol. Int.* **38**, 910 (2005).
48. W. Brostow, W. Chonkaew, L. Rapoport, Y. Soifer, and A. Verdyan: Grooves in microscratch testing. *J. Mater. Res.* **22**, 2483 (2007).
49. R.C. Desai and R. Kapral: *Dynamics of Self-organized and Self-assembled Structures* (Cambridge University Press, Cambridge—New York, 2009).
50. D. Jackovich, B. O'Toole, M. Cameron Hawkins, and L. Sapochak: Temperature and mold size effects on physical and mechanical properties of a polyurethane foam. *J. Cell. Plast.* **41**, 153 (2005).
51. S. Dalle Vacche, F. Oliveira, Y. Leterrier, V. Michaud, D. Damjanovic, and J-A. Månson: The effect of processing conditions on the morphology, thermomechanical, dielectric, and piezoelectric properties of P(VDF-TrFE)/$BaTiO_3$ composites. *J. Mater. Sci.* **47**, 4763 (2012).
52. Z. Yang, T. Chen, R. He, G. Guan, H. Li, L. Qiu, and H. Peng: Aligned carbon nanotube sheets for the electrodes of organic solar cells. *Adv. Mater.* **23**, 5436 (2011).